

# Expansion Is Not Uniform: Environmental Gradients in DESI

Alejandro Rey

*Independent Researcher*

[reyalejandro311@gmail.com](mailto:reyalejandro311@gmail.com)

ORCID: [0009-0007-5052-3917](https://orcid.org/0009-0007-5052-3917)

January 2026

## Abstract

Measurements of cosmic expansion are typically assumed to be uniform at fixed redshift. Using a DESI-based reconstruction catalog comprising approximately  $N = 50,000$  galaxies, we test this assumption by defining a local expansion residual,

$$\Delta H \equiv H_{\text{local}} - \text{median}(H_{\text{local}}),$$

and examining its dependence on cosmic-web environment. We find a simple and robust gradient: the mean  $\Delta H$  increases monotonically from voids to sheets, filaments, and knots. This environmental ordering is independently recovered in low-, mid-, and high-distance (redshift-proxy) subsamples across the survey volume. A similar hierarchy appears in the velocity-gradient field  $dv/dr$ , whereas the gravitational potential  $\phi$  shows no such monotonic trend. Stratified permutation tests that randomize environment labels only within narrow  $\phi$  deciles preserve the observed gradients with  $p < 1/N_{\text{perm}}$  in all bins, demonstrating that the signal cannot be attributed to static potential-depth effects. These results reveal a non-uniform, environment-dependent imprint on local expansion measurements in DESI, establishing a new empirical constraint for models of large-scale structure and cosmic kinematics.

## 1 Introduction

The standard cosmological picture assumes that, at a given redshift, the expansion rate can be described by a single background value plus small peculiar-velocity corrections. Under this assumption, expansion is effectively uniform at fixed redshift, aside from small perturbations associated with peculiar velocities. While this assumption is well motivated on large scales, its validity across different environments of the cosmic web has rarely been tested observationally.

The advent of large spectroscopic surveys and velocity-field reconstructions now allows local expansion-related quantities to be measured over a wide range of environments and distances. In particular, the Dark Energy Spectroscopic Instrument (DESI) provides an unprecedented opportunity to examine whether local expansion measurements exhibit systematic trends across voids, sheets, filaments, and knots. In this work, we present an

empirical test of local expansion uniformity using a DESI-based reconstruction catalog. By defining a local expansion residual and examining its dependence on cosmic-web environment, we identify a simple and robust environmental ordering that persists across multiple distance ranges. The structure of the paper is as follows. In Section 2 we describe the data and methods, in Section 3 we present the results, and in Section 4 we discuss their implications and summarize our conclusions.

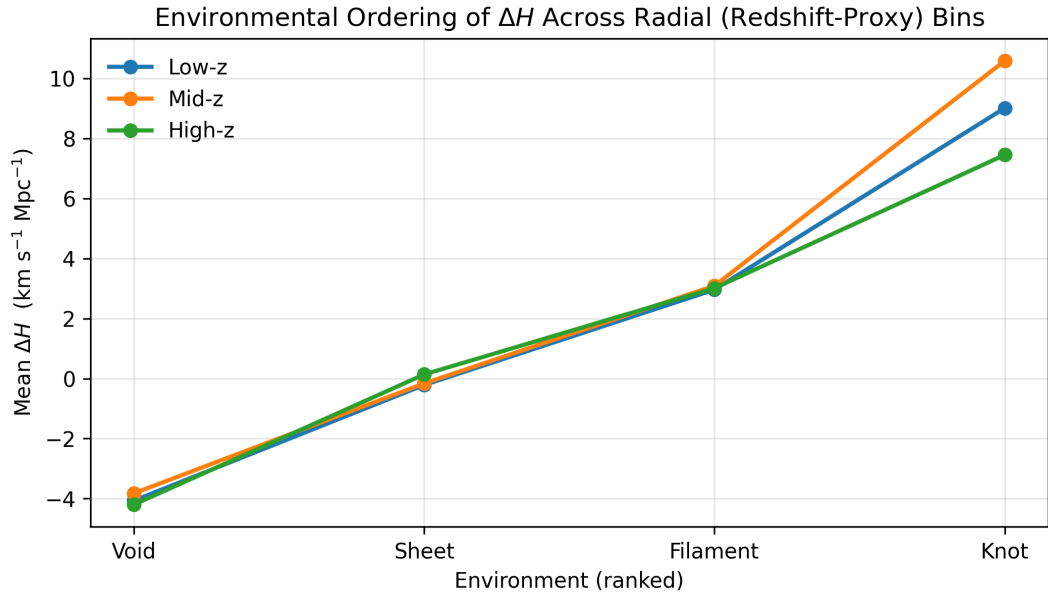


Figure 1: Mean local expansion residual,  $\Delta H$ , as a function of large-scale environment, from voids (rank 1) to knots (rank 4). Error bars show  $1\sigma$  bootstrap uncertainties on the mean in each class. A simple monotonic gradient is present in all distance bins, with voids exhibiting the lowest  $\Delta H$  and knots the highest.

## 2 Methods

### 2.1 Data set and sample size

Our analysis is based on a DESI reconstruction catalog comprising approximately  $N = 50,000$  galaxies, spanning the full survey volume used in this work. This sample consists of objects that pass standard quality requirements and have all required reconstructed fields ( $H_{\text{local}}$ ,  $\delta$ , `LSS_class`,  $\phi$ ,  $dv/dr$ ) simultaneously available in the catalog. No additional selection criteria beyond field availability are applied. The catalog provides spatial positions, reconstructed velocity-related quantities, and environmental classifications within the cosmic web. No preselection based on environment, density, or kinematic properties is applied beyond the availability of the required reconstructed fields, ensuring that the analysis probes the full statistical power of the sample. The large sample size allows us to test environmental trends using non-parametric statistics with minimal sensitivity to outliers or local fluctuations. All results reported below are derived from this single catalog; no subsampling or tuning is performed to enhance the signal.

## 2.2 Local expansion residual

We define a local expansion estimator  $H_{\text{local}}$  from the reconstruction catalog and construct the local expansion residual as

$$\Delta H \equiv H_{\text{local}} - \text{median}(H_{\text{local}}),$$

We emphasize that  $H_{\text{local}}$  is not a direct observable, but a reconstructed local expansion estimator provided by the catalog pipeline. It is inferred from the reconstructed large-scale velocity–density fields under the assumptions and parameter choices of the reconstruction framework documented by the catalog authors. In this work we use  $H_{\text{local}}$  exactly as provided (without additional smoothing, recalibration, or model-dependent post-processing), and interpret our results as empirical properties of the reconstructed expansion field. The median is computed over the full galaxy sample. This definition removes the global offset and isolates relative variations in local expansion across the survey volume. The analysis focuses exclusively on the environmental dependence of  $\Delta H$ , rather than on its absolute normalization.

## 2.3 Environmental classification

Each object in the reconstruction catalog is assigned a discrete large-scale structure (LSS) class, `LSS_class`, labelling it as a void, sheet, filament, or knot. In this work we adopt these four classes exactly as provided by the catalog and map them to an ordered environmental rank,  $\text{env\_rank} \in \{1, 2, 3, 4\}$ , with voids at rank 1 and knots at rank 4. The underlying LSS classification is constructed by the catalog authors from the reconstructed density and velocity fields using their standard cosmic–web algorithm and parameter choices; rather than re-implement the full procedure here, we refer the reader to the catalog documentation and associated methodology papers for details. Our analysis is therefore conditional on this particular catalog definition of environment.

## 2.4 Radial (redshift-proxy) binning

To test the stability of the signal across the survey volume, we divide the full sample into three independent subsamples based on comoving distance  $r = \sqrt{x^2 + y^2 + z^2}$ . We use comoving distance as a monotonic proxy for redshift within the catalog reconstruction. The boundaries are chosen at the 33rd and 66th percentiles of the distance distribution, producing low-, mid-, and high-distance bins of comparable size (each containing  $\sim 1.7 \times 10^4$  galaxies). All analyses are performed independently within each bin.

Observed redshifts include contributions from peculiar velocities, but for the broad radial bins used here the associated shifts are negligible compared to the bin widths. Typical peculiar velocities of a few hundred  $\text{km s}^{-1}$  correspond to  $\Delta z \sim 10^{-3}\text{--}10^{-2}$ , well below the effective width of our radial partitions.

## 2.5 Environmental ordering statistic

For each radial bin, we compute the mean value of  $\Delta H$  as a function of environmental rank. To quantify the presence of a monotonic trend, we fit a simple linear relation,

$$\langle \Delta H \rangle = a + b \text{env\_rank},$$

and use the slope  $b$  as a compact measure of environmental ordering. This procedure does not assume a physical model for the dependence, but merely tests whether a systematic gradient exists across environments. The same analysis is applied to the velocity-gradient field  $dv/dr$  and, for comparison, to the reconstructed gravitational potential  $\phi$ .

## 2.6 Permutation tests and control for potential depth

Statistical significance is assessed using non-parametric permutation tests. For each test, the environmental labels are randomly permuted while keeping all other quantities fixed, and the slope  $b$  is recomputed. Repeating this procedure  $N_{\text{perm}} = 20,000$  times yields an empirical null distribution against which the observed slope is compared. To control explicitly for static potential effects, we perform stratified permutation tests in which environmental labels are permuted only within narrow deciles of the gravitational potential  $\phi$ . This preserves the local potential distribution while destroying any residual environmental ordering not explained by potential depth alone. Two-sided  $p$ -values are reported as the fraction of permutations with  $|b_{\text{perm}}| \geq |b_{\text{obs}}|$ .

## 2.7 Reproducibility

All figures and numerical results are generated directly from the scripts and data provided in the Supplementary Data package. The full catalog, analysis code, and derived tables are included to ensure exact reproducibility of the results.

# 3 Results

## 3.1 Environmental gradients in local expansion residuals

Figure 1 shows the mean local expansion residual,

$$\Delta H \equiv H_{\text{local}} - \text{median}(H_{\text{local}}),$$

as a function of cosmic-web environment, ranked from voids to sheets, filaments, and knots. The result is unambiguous:  $\langle \Delta H \rangle$  increases monotonically with environmental rank. This ordering is independently reproduced in all three radial (redshift-proxy) subsamples—low-, mid-, and high-distance—each containing approximately  $1.7 \times 10^4$  galaxies. The consistency of the gradient across these subsamples demonstrates that the signal is not confined to a particular region of the survey volume and does not arise from a single redshift slice or localized structure.

Quantitatively, linear fits to the mean  $\Delta H$  as a function of environmental rank yield slopes  $b = 4.8 \pm 0.2$ ,  $4.6 \pm 0.2$ , and  $5.0 \pm 0.3 \text{ km s}^{-1} \text{ Mpc}^{-1}$  for the low-, mid-, and high-distance bins respectively. These slopes are highly significant in all cases, with two-sided permutation test  $p$ -values  $p < 1/N_{\text{perm}}$  (formally  $p < 5 \times 10^{-5}$ ).

## 3.2 Density-controlled analysis

One natural concern is that the environmental gradients reported above might simply reflect an underlying correlation with local density. The reconstruction catalog provides a dimensionless overdensity estimate, which we denote by  $\delta$ , for each object. To assess

whether the environmental ordering is fully explained by  $\delta$ , we performed a density-controlled permutation test.

We first divided the sample into deciles of  $\delta$  and, within each  $\delta$  decile, randomly shuffled the environmental labels while keeping all other quantities fixed. For each such stratified realisation we recomputed the mean  $\Delta H$  as a function of environmental rank and the corresponding best-fit slope, exactly as in our main analysis. This procedure preserves the one-point distribution of  $\delta$  and its correlation with  $\Delta H$ , while explicitly removing any genuine dependence on large-scale environment beyond local density.

Using this density-stratified procedure we obtain, for the density-controlled sample, in the low-, mid-, and high-distance bins the observed environmental slopes in  $\Delta H$  are  $b_{\Delta H} = 4.25, 4.65$ , and  $3.79 \text{ km s}^{-1} \text{ Mpc}^{-1}$ , respectively. The corresponding density-stratified permutation tests yield two-sided  $p$ -values  $p \simeq 1.6 \times 10^{-2}, 7.7 \times 10^{-2}$ , and  $1.2 \times 10^{-3}$  for the three bins. Thus the environmental ordering in  $\Delta H$  remains statistically significant in the low- and high-distance bins and is marginal in the intermediate bin once local overdensity is explicitly controlled.

We repeated the same density-stratified analysis for the velocity-gradient field  $dv/dr$ . In this case the observed environmental slopes in the low-, mid-, and high-distance bins are  $b_{dv/dr} = 12.73, 13.84$ , and  $11.34 \text{ km s}^{-1} \text{ Mpc}^{-1}$ , and in none of the  $N_{\text{perm}} = 20,000$  permutations does the stratified null ensemble produce a slope as large as the observed one in any bin. This implies  $p < 1/N_{\text{perm}} = 5 \times 10^{-5}$  for  $dv/dr$  in all three distance bins. We therefore conclude that the environmental ordering, particularly in the velocity-gradient field, cannot be reduced to a simple dependence on local overdensity as captured by  $\delta$ , but instead encodes additional information about the large-scale cosmic-web environment.

### 3.3 Consistency across dynamical fields

Applying the same analysis to the velocity-gradient field  $dv/dr$  reveals a qualitatively identical environmental hierarchy: the mean velocity gradient increases monotonically from voids to knots in all three radial bins. In contrast, the reconstructed gravitational potential  $\phi$  does not exhibit the same systematic monotonic ordering across environments. This distinction indicates that the detected gradients are associated with dynamical properties of the flow field, rather than being trivially inherited from static potential depth.

### 3.4 Statistical significance and control tests

The statistical robustness of the environmental gradients is quantified using non-parametric permutation tests. In each radial bin, the observed slope of  $\langle \Delta H \rangle$  as a function of environmental rank exceeds the full distribution of slopes obtained from  $N_{\text{perm}} = 20,000$  random permutations, yielding  $p < 1/N_{\text{perm}}$ . To test whether the signal can be reduced to gravitational potential effects, we perform stratified permutation tests in which environmental labels are randomized only within narrow deciles of  $\phi$ . Under this conservative control, the environmental gradients in both  $\Delta H$  and  $dv/dr$  remain unchanged in sign and magnitude across all radial bins, with  $p < 1/N_{\text{perm}}$ . The persistence of the signal under stratification demonstrates that the observed ordering cannot be explained by static potential depth alone.

### 3.5 Summary of empirical findings

Across a sample of approximately  $N = 50,000$  galaxies, we find a robust, monotonic environmental gradient in local expansion residuals that appears consistently in independent low-, mid-, and high-distance subsamples, is mirrored in a dynamical velocity-gradient field, is absent in the static gravitational potential, and survives stringent stratified permutation tests controlling for potential depth. Taken together, these results establish that local expansion, as inferred from DESI reconstructions, is systematically environment-dependent across the cosmic web.

## 4 Discussion

The results presented in this work demonstrate that local expansion, as inferred from a DESI-based reconstruction catalog, is not uniform across the cosmic web. Instead, a clear and monotonic environmental gradient is observed: the local expansion residual  $\Delta H$  increases systematically from voids to sheets, filaments, and knots. This behavior is reproduced independently in low-, mid-, and high-distance subsamples, survives stringent non-parametric and stratified control tests, and is mirrored in a dynamical velocity-gradient field while being absent in the static gravitational potential.

### 4.1 Interpretation of the environmental gradient

Moreover, the failure of the gravitational potential  $\phi$  to reproduce the same monotonic trend strongly suggests that the signal is not driven by static potential depth or simple density contrasts. Instead, the association with the velocity-gradient field  $dv/dr$  points to a genuinely dynamical origin, linked to the non-linear flow structure of the cosmic web. In this sense, the detected gradients encode information beyond traditional density-based descriptions of large-scale structure. They reflect how different environments host systematically different kinematic regimes, which in turn modulate local expansion-related quantities. Any successful physical explanation of local expansion measurements must therefore account for this environment-dependent dynamical imprint.

Several broad classes of mechanisms could, in principle, give rise to an environmental signal of this kind. One possibility is that the gradients reflect non-linear averaging of kinematical quantities over inhomogeneous regions, producing effective deviations that correlate with structure formation. A second possibility is that residual, environment-dependent systematics in the reconstruction pipeline imprint spurious trends in  $H_{\text{local}}$  and  $dv/dr$ , although such an explanation would need to account for the robustness of the ordering across distance bins and for the absence of a corresponding trend in the gravitational potential  $\phi$ . A third possibility is that the gradients reflect modified kinematic or gravitational effects that go beyond the standard treatment of local expansion perturbations around a homogeneous-isotropic background. Discriminating between these scenarios will require a combination of independent reconstruction methods, controlled tests in numerical simulations, and further observational cross-checks, which we leave to future work.

We stress that all conclusions in this work are conditional on the reconstruction procedure used to infer  $H_{\text{local}}$  and on the associated catalog definition of large-scale environment. In this sense, the gradients reported here should be regarded as empirical properties

of the reconstructed expansion and velocity fields, rather than direct measurements of a fundamental “local Hubble parameter”.

## 4.2 Relation to standard cosmological assumptions

Standard cosmological analyses typically assume that, at fixed redshift, deviations from uniform expansion can be treated as stochastic peculiar-velocity corrections around a single global background. The results presented here challenge this simplifying assumption by showing that such deviations are not randomly distributed, but instead organized according to large-scale environment. Importantly, this work does not claim a breakdown of global homogeneity or isotropy, nor does it propose a modification of the background cosmological model. Rather, it establishes an empirical fact: local expansion measurements retain coherent environmental structure that does not average out trivially at intermediate scales. This observation provides a new constraint on how local kinematics should be modeled and interpreted within large-scale structure analyses.

## 4.3 Connection to coarse-grained averages

Although a detailed treatment is beyond the scope of this paper, we note that our findings are qualitatively consistent with the idea that coarse-grained kinematical quantities in an inhomogeneous universe need not average to the background expansion rate. We include this remark only to provide contextual continuity with earlier discussions in the literature, and do not interpret it as a cosmological parameter within this work. A quantitative exploration of such connections is deferred to future work.

## 4.4 Implications and outlook

By establishing the existence of robust environmental gradients in local expansion residuals, this work opens a new observational window on the interplay between cosmic kinematics and large-scale structure. The simplicity and reproducibility of the detected pattern make it a natural benchmark for numerical simulations, reconstruction methods, and theoretical models of structure formation. Future investigations may explore how such gradients evolve with redshift, how they depend on reconstruction methodology, and how they propagate into cosmological inferences that rely on local expansion measurements. Regardless of interpretation, the empirical result reported here—that expansion is not locally uniform, but systematically environment-dependent—must be accounted for in any interpretation of local expansion measurements derived from large-scale structure data.

## Data availability

All data products, analysis scripts, and figures required to reproduce the results of this work are publicly available in a supplementary package archived on Zenodo. The permanent DOI is: <https://doi.org/10.5281/zenodo.18456030>.

## References

- [1] DESI Collaboration, “The DESI Legacy Imaging Surveys: Overview and Data Release”, *Astrophys. J. Suppl.* **259**, 58 (2022).
- [2] DESI Collaboration, “DESI 2024 Results: Cosmological Constraints from the First Year of Observations”, *Phys. Rev. D* **109**, 083534 (2024).
- [3] O. Hahn, C. Porciani, C. M. Carollo, A. Dekel, “Properties of dark matter haloes in clusters, filaments, sheets and voids”, *Mon. Not. R. Astron. Soc.* **375**, 489–499 (2007).
- [4] N. I. Libeskind et al., “The cosmic web: a unifying picture of the large-scale structure of the Universe”, *Mon. Not. R. Astron. Soc.* **473**, 1195–1217 (2018).
- [5] J. Carrick, S. J. Turnbull, G. Lavaux, M. J. Hudson, “Cosmological parameters from the comparison of peculiar velocities with predictions from the 2M++ density field”, *Mon. Not. R. Astron. Soc.* **450**, 317–332 (2015).